*Journal of the Korean Chemical Society*
**2010**, *Vol. 54, No. 1*
Printed in the Republic of Korea
DOI 10.5012/jkcs.2010.54.01.013

# 7 Diethylaminocoumarin (DEAC) 레이저 염료의 광물리적 파라미터, 광분해, 형광 소광 및 Convolutive Voltammetry

**S. A. El-Daly and I. S. El-Hallag***
Chemistry Department, Faculty of Science, Tanta University, Tanta, 31527, Egypt
(접수 2009. 8. 17; 수정 2009. 12. 29; 게재확정 2010. 1. 6)

# Photophysical Parameters, Photodecomposition, Fluorescence Quenching and Convolutive Voltammetry of 7-Diethylaminocoumarin (DEAC) Laser Dye

**S. A. El-Daly and I. S. El-Hallag***
*Chemistry Department, Faculty of Science, Tanta University, Tanta, 31527, Egypt*
**E-mail: ielhallag@yahoo.co.uk*
(Received August 17, 2009; Revised December 29, 2009; Accepted January 6, 2010)

**요약.** 7 diethylaminocoumarin (DEAC) 레이저 염료의 광물리적 특성들을 다양한 용매에서 측정하였다. DEAC의 방출 스펙트럼은 양이온성(CTAC) 미셀과 음이온성(SDS) 미셀에서 측정하였고, 레이저 파라미터는 아세톤, 다이옥산, 에탄올 및 dimethylforamide (DMF)과 같은 여러 가지 용매에 대하여 계산하였다. DEAC의 광반응성은 366 nm 빛을 사용하여 $CCl_4$ 용매에서 연구하였고, 광화학 수득률 ($\phi_c$)과 속도 상수(k)도 결정하였다. picric acid (PA), tetracyanoethylene (TCNE), 7,7,8,8-tetracynoquinonedimethane (TCNQ)등의 유기 수용체와 DEAC의 상호 작용에 대한 연구는 acetonitrile ($CH_3CN$) 용액에서 형광을 측정하므로 써 수행하였다. DEAC의 전기화학적 연구는 백금 전극을 사용하여 0.1 mol/L tetrabutyl ammonium perchlorate (TBAP)/$CH_3CN$ 용액에서 순환 전류-전압법, convolutive voltammetry 및 디지털 시뮬레이션을 조합하여 수행하였고, 전기화학 파라미터도 결정하였다.

**주제어:** 광물리적 파라미터, 형광, 레이저 파라미터, Convolutive voltammetry, 전기화학적 파라미터

**ABSTRACT.** The photophysical properties of 7-diethylaminocoumarin (DEAC) laser dye have been measured in different solvents. The emission spectrum of DEAC has also been measured in cationic (CTAC) and anionic (SDS) micelles. The laser parameters have been calculated in different solvents namely acetone, dioxane, ethanol and dimethylforamide(DMF). The photoreactivity of DEAC has been studied in $CCl_4$ solvent using 366 nm light. The values of photochemical yield ($\phi_c$) and rate constant (k) are determined. The interaction of organic acceptors such as picric acid (PA), tetracyanoethylene (TCNE) and 7,7,8,8-tetracynoquinonedimethane (TCNQ) with DEAC are also studied using fluorescence measurements in acetonitrile ($CH_3CN$). The electrochemical investigation of (DEAC) has been carried out using cyclic voltammetry and convolutive voltammetry combined with digital simulation technique at a platinum electrode in 0.1 mol $L^{-1}$ tetrabutyl ammonium perchlorate (TBAP) in $CH_3CN$ solvent. The electrochemical parameters of the investigated compound were determined using cyclic and convolutive voltammetry. The extracted electrochemical parameters were verified and confirmed *via* digital simulation method.

**Keywords:** Photophysical parameters, Fluorescence, Laser parameters, Convolutive voltammetry, Electrochemical parameters

## INTRODUCTION

Derivatives of 1,2-benzopyrone, commonly known as the coumarine dyes, are well-known laser dyes for the blue-green region.[1-8] Among these dyes, the ones having different amino groups at 7-position (commonly known as 7-aminocoumarins) are of special significations.[1-13] The fluorescence quantum yield ($\phi_f$) of these dyes is usually very high, often close to unity.[1-13] These dyes undergo substantial changes in their dipole moment upon excitation, causing large Stokes shifts between their absorption and fluorescence spectra.[1-14] Which are very sensitive to solvent polarities.[1-15] Because of these properties, the 7-aminocoumarin dyes have been widely used as probes in a variety of investigation, namely, in the study of solvatochromic properties[9-13] determination of polarities in microenvironments,[14,15] measurements of solvent relaxation times.[16-21] In the literature, it is reported that the coumarin dyes with 7-dialkylamino groups behave unusually in higher polar solvents, showing drastic reduction in their fluorescence quantum yield and fluorescence lifetime values.[9-13] Twisted intramolecular charge transfer (TICT)

states have been invoked to explain these results in higher polarity solvents.

On the other hand, study of the electrochemical reduction of coumarin has been started by Harle[22] and Capka.[23] Zuman[24-26] have reported a half-wave potential and substituents effect for coumarin derivatives and Gourley[27] have obtained the result that coumarin derivative becomes dihydrocoumarins by the electrochemical reduction in the presence of tertiary amine coumarin. Reddy[28] have suggested a polarographic reaction mechanism of 3-acetyl coumarin and Partridge,[29] Bond[30] have explained a phenomenon that coumarin becomes adsorbed to mercury electrode. Helin[31] have reported the electrochemiluminescence of 4-methyl coumarin derivatives induced by hot electrons into aqueous electrolyte solution. Diez[32] have surveyed the voltammetric determination of coumarin in the emulsified media and Wang[33] have done a differential pulse voltammetric determination with 7-hydroxy coumarin of human urine. Wang[34] have made an amperometric biosensor by modifying antibody of 7-hydroxy coumarin with glassy carbon electrode, and have investigated antibody specificity and antibody-antigen interaction kinetic. 7-hydroxy coumarins were studied using cyclic voltammetry, differential pulse voltammetry and chronocoulometry. The results showed that the coumarins undergo a pH-dependent, irreversible oxidation with product adsorption.[35]

In the present work, photophysical properties, laser parameters, fluorescence quenching and photoreactivity of DEAC have been investigated. Also, in this article, we have studied the electrochemical reduction of DEAC laser dye by cyclic voltammetry (CV), convolutive voltammetry combined with digital simulation technique.

## EXPERIMENTAL DETAILS

Laser-grade DEAC dye was obtained from Fluka and used without further purification. The organic solvents used were of spectroscopic grade. Picric acid (Aldrich) was recrystallized from ethanol, TCNE and TCNQ (Aldrich) was purified by sublimation, sodium dodecyl sulphate (SDS, Fluka) was used to prepare anionic micelles and cetyltrimethylammonium chloride (CTAC, Fluka) to prepare cationic micelles. UV-Visible electronic absorption spectra were recorded on a Shimadzu UV-160 A spectrophotometer and the steady state fluorescence spectra were measured using Shimadzu RF 510 spectrofluorophotometer. The fluorescence spectra were corrected for the machine response using $10^{-5}$ mol $L^{-1}$ anthracene solution in benzene.[36] The fluorescence quantum yield ($\phi_F$) was measured relative to 9,10-diphenylanthracene, according to the following equation:[37]

$$\Phi_f(s) = \Phi_f(r)\frac{D_s}{D_r} \times \frac{A_r}{A_s} \times \frac{n_s^2}{n_r^2}$$

Where D represents the corrected fluorescence peak area, A is the absorbance at excitation wavelength, and n is the refractive index of solvent used. The subscripts 's' and 'r' refer to sample and reference, respectively. All measurements were made at very low concentration of dye ($< 1 \times 10^{-5}$ mol $L^{-1}$) to avoid re-absorption of emitted photons. The photochemical quantum yields were calculated using method that was described in details previously.[38] The light intensity was measured by using ferrioxalate actinometry.[39] The laser action of DEAC using GL-302 dye laser, pumped by a nitrogen laser (GL-3300 nitrogen laser, PTI). The pump laser ($\lambda$ = 337.1 nm) was operated at repetition of 3 Hz with a pulse energy of 1.48 mJ and pulse duration rate of 800 ps. The narrow-band output of the dye laser was measured with pyroelectric Joule meter (ED 200, Gen-Tec Inc.).

Cyclic voltammetry measurements are made using a conventional three electrode cell configuration linked to an EG & G model 170 PAR apparatus. The platinum electrode surface was $1 \times 10^{-4}$ $m^2$ as a working electrode, silver-silver chloride as a reference electrode, coiled platinum wire as a counter electrode and 0.1 mol $L^{-1}$ tetrabutyl ammonium perchlorate (TBAP) as background electrolyte. Cyclic voltammograms were recorded after background subtraction and iR compensation to minimize double-layer charging current and solution resistance. The working electrode was polished on a polisher Ecomet grinder. Cyclic voltammetric data were obtained at scan rates ranging from 0.02 to 5 V $s^{-1}$ in non aqueous media at 22 ± 2 °C. Digital simulation of the data for cyclic voltammetric experiments were carried out on a PC computer using EG & G condesim package. Convolution-deconvolution voltammetry was performed using EG & G condecon software package. All working solutions were thoroughly degassed with oxygen free nitrogen and a nitrogen atmosphere was maintained above the solution throughout the experiments.

## RESULTS AND DISCUSSION

### Solvent polarity effect on absorption and fluorescence spectra

Absorption and fluorescence spectra of DEAC dye are strongly dependent on solvent polarities (*Fig*. 1). *Table* 1 lists the photophysical parameters such as $\lambda_{abs}$ (max), $\lambda_{em}$ (max), and fluorescence quantum yield along with solvent polarity function ($\Delta$f). The spectral shifts in absorption are generally found to be smaller than those found in fluorescence emission implying a greater dipole moment (polarity) of the dye in the excited state compared to that in the ground state. This is also in agreement with $\pi,\pi^*$ nature of the lowest singlet excited state of DEAC. The marginal deviation in data points for alcoholic solvents are assigned to solute-solvent hydrogen bonding

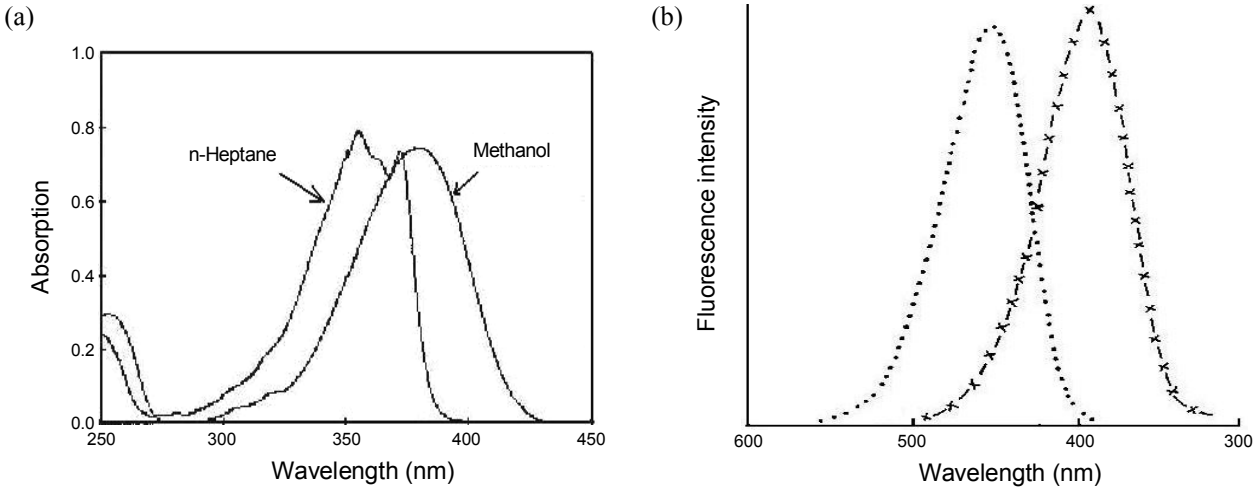


*Fig*. 1. (a) Electronic absorption spectrum of $3 \times 10^{-5}$ mol $dm^{-3}$ of DEAC n-heptane and MeOH. (b) Emission spectrum of DEAC in (---x---) MeOH and (…) n-hexane.

*Table* 1. Photophysical properties of DEAC in different solvents

| Solvents | Photophysical properties | | | | | |
|---|---|---|---|---|---|---|
| | $\Delta f$ | $\lambda_{ab}$ (nm) | $\lambda_{em}$ (nm) | $\Delta\upsilon$ ($cm^{-1}$) | $\phi_f$ | Ma (Debye) |
| n-Hexane | 0.0 | 353 | 392 | 2817 | 0.85 | 10.8 |
| n-Heptane | 0.0002 | 352 | 390 | 2768 | 0.85 | 10.8 |
| Benzene | 0.0052 | 355 | 395 | 2853 | 0.83 | 10.4 |
| Toluene | 0.0133 | 369 | 418 | 3177 | 0.83 | 10.3 |
| Diethyl ether | 0.166 | 359 | 405 | 3164 | 0.80 | 10.5 |
| $CCl_4$ | 0.008 | 360 | 412 | 3505 | --- | 10.2 |
| $CHCl_3$ | 0.233 | 375 | 435 | 3677 | 0.62 | 9.6 |
| DMF | 0.274 | 379 | 440 | 3657 | 0.56 | 9.4 |
| n-Propanol | 0.277 | 379 | 442 | 3760 | 0.52 | 8.85 |
| Acetone | 0.284 | 370 | 430 | 3771 | 0.55 | 10.7 |
| EtOH | 0.290 | 380 | 443 | 3742 | 0.39 | 8.6 |
| MeOH | 0.309 | 381 | 445 | 3775 | 0.27 | 8.62 |
| Ethylene glycol | 0.30 | 381 | 445 | 3775 | 0.25 | --- |
| n-Butanol | 0.263 | 379 | 442 | 3376 | 0.47 | --- |

interaction, which causes an extra red shift in the observed spectra.[40-42]

Analysis of the solvatochromic behavior allows to estimate the difference in the dipole moment between the excited singlet and the ground state ($\Delta\mu_e - \Delta\mu_g$). This was achieved by applying the simplified Lippert-Mataga equation.[43-45]

$$\Delta\nu_{st} = \Delta\nu_o + \frac{2\left(\mu_e - \mu_g\right)^2}{hca^3}\Delta f$$

$$\Delta f = \frac{\varepsilon - 1}{2\varepsilon + 2} - \frac{n^2 - 1}{2n^2 + 1}$$

Where $\Delta\upsilon_{st}$ is the Stokes-shift (in $cm^{-1}$), which increases with increasing solvent polarity pointing to stronger stabilization of excited state in polar solvents, h is the Planck's constant, *c* is the velocity of light and *a* is the Onsager cavity radius, ε and n are the dielectric constant and refractive index of the solvent, respectively. The Onsager cavity radius *a* was calculated from the energy minimized structures obtained with the AM1 calculation. It defined as the radius of the spherical cavity surrounding the molecular van der Waals radius. The maximum distance where charge separation can occur across the molecule must be considered, rather than the actual molecular axis of the molecule.[46] For DEAC this distance lies between the average coordinates of the nitrogen atoms on one side of the molecule and the oxygen atom in the other side of the molecules it was estimated to 9.0 Å , the cavity radius *a* was taken as half of this distance that is 4.5 Å. *Fig*. 2 shows the plot of Stokes shift versus the orientation polarization (Δf). The change of dipole moment upon excitation which was calculated from slope of the plot and the cavity radius is 4.76 Debye, indicating the polar nature of the fluorescent states. We assign this state to be of intramolecular charge transfer (ICT) character. In the earlier work, a similar ICT character was assigned to the fluorescent states of 7-amino coumarin derivatives.[8-12]

The fluorescence quantum yield ($\phi_f$) values of DEAC were estimated in different solvents at room temperature and listed in *Table* 1. *Fig*. 3 shows the plot of $\phi_f$ versus Δf. The interesting point from this plot is that the $\phi_f$ values reduce in higher polarity solvents, having $\Delta f > 0.2$. In lower medium polarity solvent region ($\Delta f < 0.2$), however, $\phi_f$ reduces only marginally with Δf following apparently a linear correlation indicated that the dye exist in ICT structure in these solvents. Thus the drastic reduction in the $\phi_f$ values above $\Delta f \cong 0.2$ clearly indicates that in the higher polarity solvents**,** the excited state of the dye undergoes

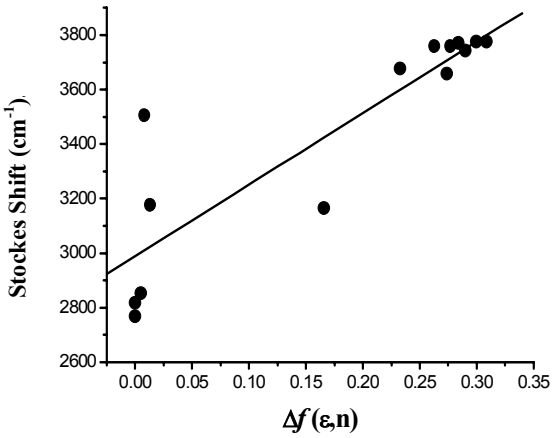


*Fig*. 2. Plot of Stokes shift ($\Delta\upsilon$ in $cm^{-1}$) for DEAC against the solvent polarity function ($\Delta f$).

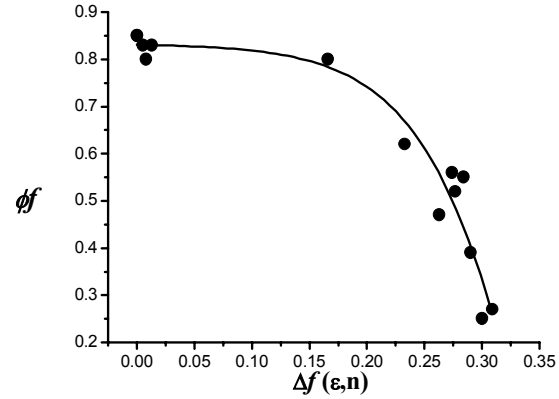


*Fig*. 3. Plot of fluorescence quantum yield ($\phi_f$) of DEAC versus solvent polarity ($\Delta f$).

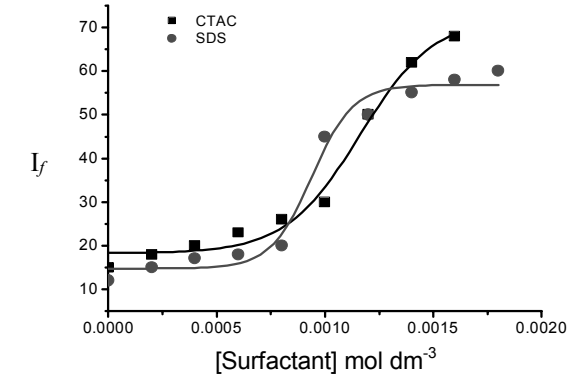


*Fig*. 4. Emission intensity of $1 \times 10^{-5}$ mol $dm^{-3}$ DEAC in different concentrations of SDS and CTAC ($\lambda_{ex}$= 337 nm).

a fast non-radiative deexcitation process due to stabilization of twisting intramolecular charge transfer (TICT) non-emissive state, which is absent in lower medium polarity of solvents.[45]

The transition dipole moment ($M_a$) of DEAC from ground to excited state was calculated in different solvents from the absorption spectrum using the simplified expression;[40, 47, 48]

$$M_a = 0.0958\ (\varepsilon_{max}\ \Delta\upsilon_a^{1/2}\upsilon_a)^{0.5}$$

Where $\varepsilon_{max}$ is the maximum value of molar absorption coefficient of the absorption band with a maximum at $\upsilon_a$ and full width at half maximum of $\Delta\upsilon_a^{1/2}$, the values of $M_a$ are listed in *Table* 1.

The emission spectrum of $1 \times 10^{-5}$ mol $L^{-1}$ of DEAC has also been measured in CTAC and SDS micelles media, as shown in *Fig*. 4. The emission intensity of dye increases as the concentration of surfactants increase, an abrupt change in the fluorescence intensity is observed at surfactant concentration of $1 \times 10^{-4}$ and $8 \times 10^{-3}$ mol $L^{-1}$ which is very close to the critical micelle concentration of CTAC and SDS, respectively.[49, 50]

**Laser parameters of DEAC**

DEAC has high fluorescence quantum yield, high molar absorptivity and high photostability in most organic solvents. In addition, the dye is free from molecular aggregation both in ground and in the excited state since the emission spectrum suffers no shift as the concentration is raised up to $5 \times 10^{-3}$ mol $L^{-1}$. Solution of $2 \times 10^{-3}$ mol $L^{-1}$ in different solvents namely acetone, dioxane, DMF and ethanol give laser emission upon pumping by nitrogen laser ($\lambda_{ex}$ = 337.1 nm) of 800 ps duration rate and 1.48 mJ pulse energy. The dye solution was taken in oscillator and amplifier cuvetts of 10 mm path length. The output energy of laser dye was measured as a function of wavelength to determine the lasing range in different solvents. The gain coefficient α (λ) of laser emission of DEAC was calculated by measuring the intensity of laser emission from the entire cell length and that from the cell half-length ($I_L$ and $I_{L/2}$, respectively) according to the following relation:[51]

$$\alpha(\lambda) = \frac{2}{L}\ln\left[\frac{I_L}{I_{L/2}} - 1\right]$$

The cross section for stimulated laser emission $\sigma_e$ was calculated at laser emission maximum according to the equation;[51]

$$\sigma_e = \frac{\lambda_e^4 E(\lambda)\Phi_f}{8\pi c n^2 \tau_f}$$

Where $\sigma_e$ is the emission wavelength, n is the refractive index of solution, c is the velocity of light and E (λ) is the normalized fluorescence line-shape function. This is correlated with fluorescence quantum yield by the equation;[52]

$$\int E(\lambda)d\lambda = \Phi_f$$

*Table* 2. Laser parameters of DEAC laser dye

| Solvent | Laser parameters | | | | |
|---|---|---|---|---|---|
| | Lasing rang | λ (max) (nm) | α ($cm^{-1}$) | $\sigma_e \times 10^{16}$ $cm^2$ | $E_{1/2}$ J/L |
| Acetone | 415-451 | 430 | 2.2 | 1.6 | 7400 |
| Dioxane | 405-450 | 425 | 1.8 | 1.45 | 13333 |
| EtOH | 425-465 | 440 | 1.74 | 1.5 | 14800 |
| DMF | 420-45 | 438 | 2.4 | 1.65 | 15564 |

E (λ) is obtained from solution whose absorbance is low to avoid reabsorption processes (optical density at absorption maximum < 0.1).

The values of α (λ) and $\sigma_e$ at maximum laser emission are listed in *Table* 2. The photochemical stability of DEAC laser dye was determined as half-life energy ($E_{1/2}$)[53] which is the amount of total absorbed pump energy until the dye laser energy has dropped to 50% of its output initial value. By knowing the concentration of the laser dye and photon energy of nitrogen laser used the $E_{1/2}$ value was calculated in term of Joule per liter of solution (*Table* 2).

**Photoreactivity of DEAC in carbon tetrachloride solvent**

The photoreactivity of DEAC has been studied in carbon tetrachloride ($CCl_4$) upon irradiation of $2 \times 10^{-5}$ mol $L^{-1}$ solution of DEAC by 366 nm light ($I_o = 3.6 \times 10^{-6}$ Ein/min). The absorbance of DEAC decreases with increasing the radiation time and two isobestic points appear at 325 and 385 nm indicating the presence of two photoproducts. The two new absorption peaks appear at 410 nm and 280 nm corresponding to the absorption of contact ion pair which has large dipole moment and to the absorption of trichloromthyl radical as shown in *Fig*. 5. The net photochemical quantum yield ($\phi_c$) of the underlying reaction was calculated as 0.054. The formation of photoproduct is a one photon process and represented by the following scheme as reported earlier[54-60] for some aliphatic and aromatic amine and also for aromatic hydrocarbon such as anthracene and perylene derivatives.

$$DEAC + h\nu \rightarrow {}^1(DEAC)^* \quad \text{absorption of light} \cdots\cdots\cdots 1$$

$${}^1(DEAC)^* \rightarrow DEAC + h\nu \quad \text{fluorescence} \cdots\cdots\cdots\cdots 2$$

$${}^1(DEAC)^* + CCl_4 \rightarrow {}^1[DEAC^{+\delta}\ldots{}^{-\delta}CCl_4]^* \quad \text{exciplex} \cdots 3$$

$${}^1[DEAC^{+\delta}\ldots{}^{-\delta}CCl_4]^* \rightarrow DEAC^{\cdot+} + {}^{\cdot-}Cl + {}^{\cdot}CCl_3 \cdots\cdots\cdots 4$$

It was proposed that the electron transfer from excited singlet DEAC* to $CCl_4$ within transient excited charge transfer complex is the main primary photochemical process (step 3). It leads to the DEAC radical cation, a chloride ion and a trichloromethyl radical in solvent cage (step 4). The formation of

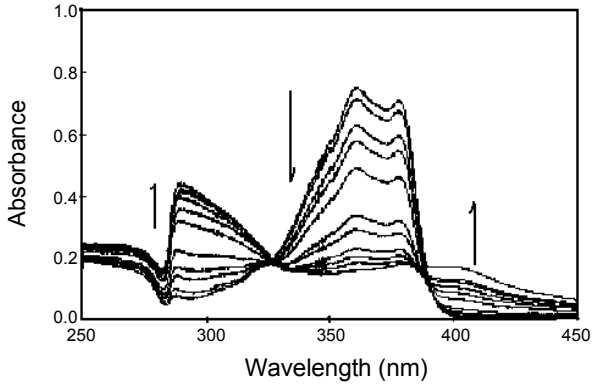


*Fig*. 5. (a) effect of irradiation on electronic absorption spectrum of $2 \times 10^{-5}$ mol $dm^{-3}$ of DEAC ($\lambda_{ex}$ = 365nm, $I_o = 3.6 \times 10^{-6}$ Ein/min). The irradiation times at decreasing absorption are 0.0, 3, 7, 10, 15, 20, 26, 26, 32, 40, 45, and 50 min.

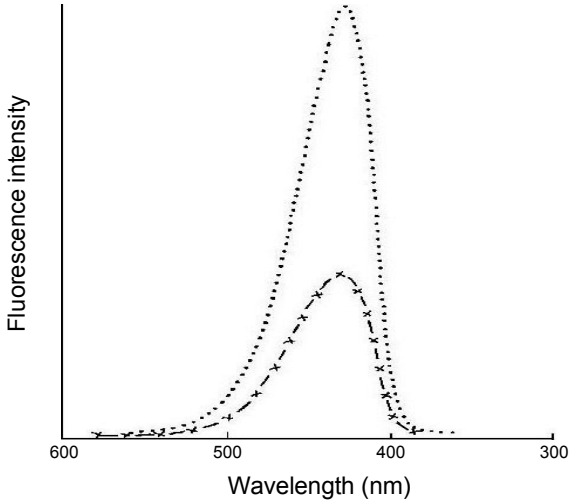


*Fig*. 6. Emission spectrum of $1 \times 10^{-5}$ mol $dm^{-3}$ of DEAC in absence (--x--) and presence (....) of $1.4 \times 10^{-4}$ mol $dm^{-3}$ of picric acid ($\lambda_{ex}$ = 337 nm).

a contact ion pair [$DEAC^{+\cdot}\ldots{}^{\cdot}Cl$] usually occurs by electron transfer from excited donor molecule to acceptor. In order to such compound to be formed a low ionization potential of donor and high electron affinity of acceptor are necessary.

The rate constant of photodecomposition of DEAC was calculated by applying the simple first order rate equation as follow:

$$\ln \frac{A_o - A_\infty}{A_t - A_\infty} = kt$$

Where $A_0$, $A_t$ and $A_\infty$ are the initial absorbance, absorbance at time (t) and infinity, respectively. k is the rate constant. The rate constant was found to be 0.067 $min^{-1}$.

It worthwhile to mention that the DEAC is highly photostable in polar solvents.

**Fluorescence quenching by organic acceptors**

The fluorescence quenching of $1 \times 10^{-5}$ mol $L^{-1}$ DEAC are also studied in acetonitril solvent using organic acceptors such as picric acid (PA, $E_A = 0.7$ eV), TCNE ($E_A = 1.7$ eV) and TCNQ ($E_A = 2.2$ eV). It was observed that the absorption spectrum when taken with increasing concentration of acceptor does not show any shift in wavelength. There is no additionally peak appearing, hence there could not be any ground state interaction between DEAC and acceptors. The emission spectrum of DEAC shows (i) no change in fluorescence spectra other than diminishing fluorescence intensity with increasing quencher concentration, (ii) no appearances of any new band at longer wavelength as shown in *Fig*. 6, this shows the absence of emissive exciplex and (iii) the Stern-Volmer plot for the fluorescence quenching of DEAC by organic acceptor is linear (*Fig*. 7). The Stern-Volmer equation is given by:

$$\frac{I_o}{I} = 1 + k_{sv}[Q]$$

Where $I_o$ and I are the fluorescence intensities in the absence and presence of the quencher [Q], $K_{sv}$ is the Stern-Volmer rate constant obtained from the slope. For dynamic quenching $K_{sv} = k_q\tau_f$ where $k_q$ is the bimolecular quenching rate constant ($M^{-1}$ $s^{-1}$) and $\tau_f$ is the excited singlet lifetime of fluorophore in the absence of quencher. For DEAC $\tau_f$ is 2.25 ns, the bimolecular quenching rate constants $k_q$ were calculated as $5.3 \times 10^{12}$, $8.8 \times 10^{12}$ and $1.5 \times 10^{13}$ $M^{-1}s^{-1}$ for PA, TCNE and TCNQ, respectively, indicating that the fluorescence quenching rate constant increases with increasing the electron affinity of acceptor. The effect of temperature of fluorescence quenching of DEAC by picric acid was also studied in the range 25 - 60 °C. The activation energy $E_a$ associated with $k_q$ was calculated assuming the Arrhenius equation to be valid for $k_q$:

$$k_q = A\exp(-E_a / RT)$$

The value obtained is 9.8 kJ $mol^{-1}$, which is very close to the activation energy associated with solvent viscosity ($E\eta$ = 10 - 13 kJ $mol^{-1}$), indicating a diffusion mechanism for fluorescence quenching (dynamic quenching mechanism). Thus, we infer that quenching of DEAC by organic acceptor proceed predominantly *via* a non-emissive exciplex with charge transfer occurring from the excited fluorophore to acceptor according to the following scheme.[61]

$$D^*\ldots A \leftrightarrow D^*A \rightarrow [DA]^* \rightarrow D^{+\cdot}A^{-\cdot} \rightarrow D^{+\cdot}\ldots A^{-\cdot} \rightarrow D^{+\cdot} + A^{-\cdot}$$

Encounter collision exciplex contact solvent separated free ions

Complex complex ion pair ion pair

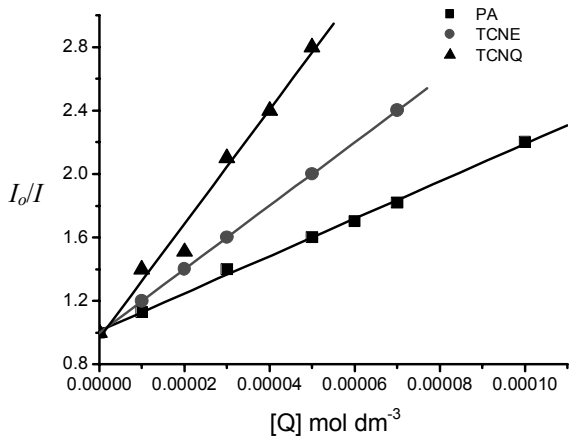


*Fig*. 7. Stern-Volmer plots for fluorescence quenching of $1 \times 10^{-5}$ mol $dm^{-3}$ of DEAC in $CH_3CN$ using PA, TCNE and TCNQ ($\lambda_{ex}$ = 337 nm).

A molecular orbital wave function representation is used to express the electronic interaction in an exciplex a summation of possible state[47] (when ground-state interaction are neglected).

$$\Psi = c_1\psi(D^*A) + c_2\psi(DA)^* + c_3\psi(D^{+\cdot}A^{-\cdot})$$

If $c_3 >> c_2$, the exciplex has pronounced charge-transfer character and will have a tendency to dissociate into radical ion pairs, especially in polar solvents. In the extreme case, an exciplex is more accurately described as a contact ion pair. Emission from exciplexes proceeds by a vertical, Franck-Condon allowed transition from a minimum on an excited-state surface to a low lying repulsive ground-state surface. If the transition to the low lying repulsive ground state involves a significant nuclear change, then emission may not be observed. Other decay processes, such as ionic dissociation into solvent-separated radical ions or chemical reactions may prevail.[61] For $c_3 << c_2$, exciplex formation leads to energy transfer. In such a case, exciplexes tend to emit light or undergo separation to form the excited state of the acceptor and ground state of donor.

The absence of static quenching of DAEC by organic acceptor is indicated from the following observation (i) the absorption spectrum of the fluorophore shows no change in the presence of the quencher. (ii) No excitation wavelength dependence of $k_q$ was observed, (iii) Stern-Volmer plot is linear and (iv) the quenching rate constant increase with increasing the temperature.

**Cyclic Voltammetry study**

Cyclic voltammetry of the reductive process of the laser dye compound, DEAC, was measured in $CH_3CN$, solvent, at scan rates ranging from 0.02 - 5 $Vs^{-1}$. The cyclic voltammogram shown in *Fig*. 8 exhibited two reductive peaks coupled with

*Table* 3. Electrochemical parameters of the reduction process of DEAC laser dye

| Technique | Electrochemical Parameters | | | | | | | |
|---|---|---|---|---|---|---|---|---|
| | $-E_1^o$ V | $-E_2^o$ V | $k_{s1} \times 10^5$ m s$^{-1}$ | $k_{s2} \times 10^5$ m s$^{-1}$ | $D_1 \times 10^{10}$ m s$^{-1}$ | $D_2 \times 10^{10}$ m s$^{-1}$ | $\alpha_1$ | $\alpha_2$ |
| CV | 1.520 | 1.680 | 2.30 | 1.50 | 4.50 | 4.85 | 0.35 | 0.32 |
| Conv | --- | --- | --- | --- | 4.60 | 4.79 | --- | --- |
| Decon | 1.510 | 1.690 | --- | --- | 4.46 | 4.46 | --- | --- |
| Sim | 1.513 | 1.675 | --- | --- | 3.23 | 3.54 | --- | --- |

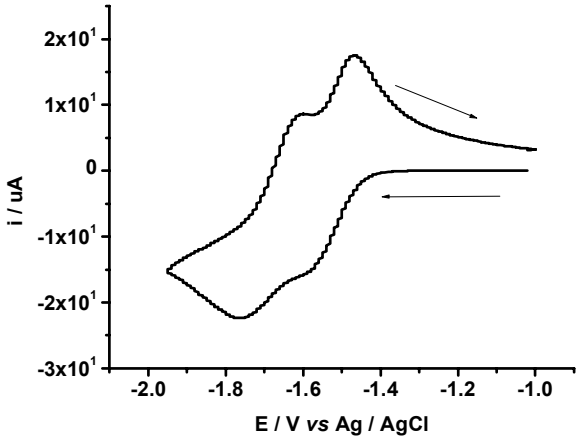


*Fig*. 8. Cyclic voltammogram of DEAC at sweep rate of 0.1 Vs $^{-1}$.

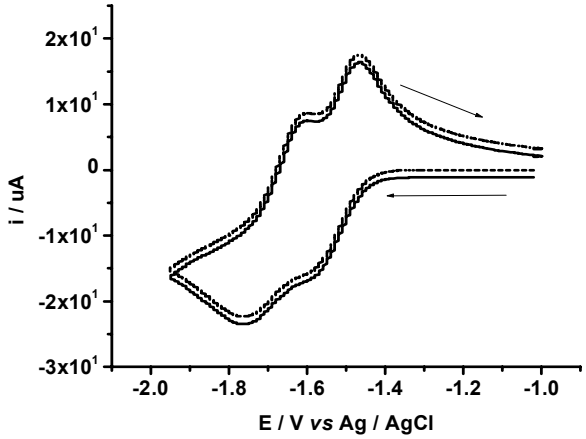


*Fig*. 9. Matching between experimental (——) and simulated (------) voltammograms of DEAC at sweep rate of 0.1 Vs $^{-1}$.

two anodic peaks. It was found that the peak currents increase with increasing the scan rate, while the cathodic peak potentials of the reduction process are dependent on the scan rate. From cyclic voltammetric investigation, it was found that, the cathodic reduction process of the investigated DEAC laser dye proceeded as a simple moderate fast charge transfer at all sweep rates. This behaviour demonstrates that the first charge transfer of the first peak produces a radical anion which gains another electron to form a dianion in the second peak. *Fig*. 8. Gives an example of the cyclic voltammogram at sweep rate of 0.1 Vs $^{-1}$ of the compound DEAC. It was observed that the forward peak potentials ($E_{pf}$) shift to more negative potential with increasing the sweep rate confirming the moderate rate of electron transfer. In the selected media, the first and the second reductive peaks were coupled with the oxidative peaks in the reverse scan. The ratio of the backward peak to the forward peak ($i_{pb}/i_{pf}$) equals to one for the two peaks, confirming the absence of chemical step, i.e., the electrode reaction behaves as EE scheme.

The reduction peak current, after elimination of the background current, is proportional to the square root of the scan rate ($v^{1/2}$) and the difference between the forward and backward peak potentials, $\Delta E_p$, is dependent on the value of the scan rate ($v$) used. The measured values of peak width $E_p - E_{p/2} = 76.5/n$ mV ± 2 and 81/n mV ± 2 at scan rate of 0.1 Vs$^{-1}$ for the first and the second peak respectively demonstrate the quasireversibile behaviour of the system, where $E_p$, $E_{p/2}$ and n are the peak potential, the half peak potential and the number of electrons respectively. At scan rate of 0.2 Vs$^{-1}$ the peak separation $\Delta E_p$ of the first charge transfers was found to be 110 mV while for the second peak is 115 mV confirming the moderate fast of charge transfer in 0.1 mol L$^{-1}$ TBAP/$CH_3CN$. The redox potential ($E^{o'}$) was determined from the mean position of the peak potentials (*Table* 3). The standard heterogeneous rate constant ($k_s$) was extracted from the cyclic voltammograms *via* peak separation using a table of $\Delta E_p$ values *vs*. heterogeneous rate constants.[62] In this case, the peak current $i_p$, is governed by the Randle-Sevcik relationship.[63] From the plot of $i_p$ *vs*. $\sqrt{v}$, the diffusion coefficient ($D$) of the electroactive species was determined. The calculated values of $D$ are cited in *Table* 3. A direct test of the experimental electrochemical parameters was verified *via* matching of the generated **cyclic** voltammograms with the experimental one using the average experimentally determined values of $k_s$, $D$ and $E^{o'}$ cited in *Table* 3 for a symmetry coefficient ($\alpha$) of 0.32 ± 0.01 which determined from digital simulation. The results given in *Fig*. 9 employ the experimental and theoretical values of the electrochemical parameters of the compound DEAC, which demonstrate good agreement between the captured and the simulated data.

Convolutive voltammetry has been successfully applied to analysis of mechanism of several electrochemical processes.[64-73] Convolution of the current with an inverse square root of time function was defined as:[65-70]

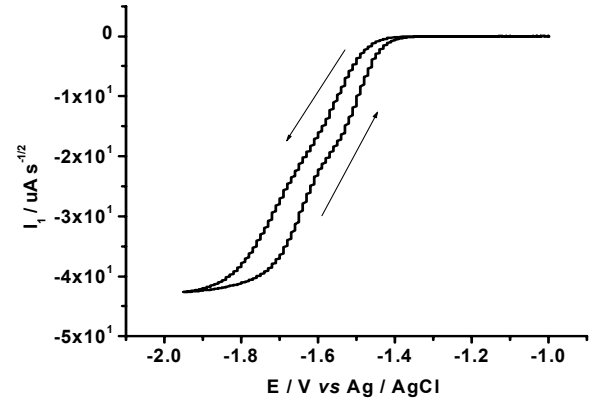


*Fig*. 10. $I_1$ convolution of DEAC at sweep rate of 0.1 $Vs^{-1}$.

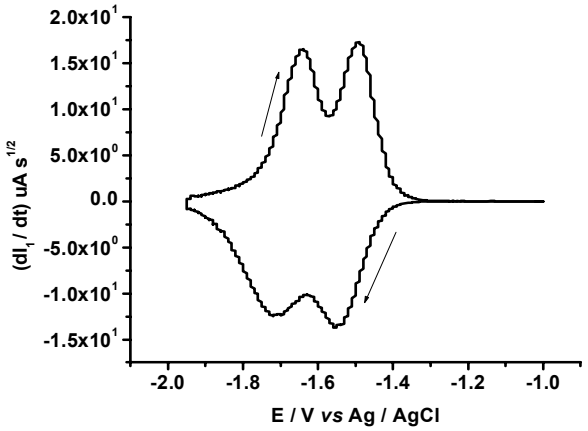


*Fig*. 11. Deconvolution voltammogram of DEAC at sweep rate of 0.1 $Vs^{-1}$.

$$I_1 = \frac{1}{(\pi)^{0.5}} \int_0^t \frac{i(u)}{(t-u)^{0.5}}\, du \tag{5}$$

where $I_1$ is the convoluted current at the total elapsed time ($t$), $i(u)$ is the experimental current at time $u$. The diffusion coefficient of the investigated complex was determined, after applying background subtraction and correction for uncompensated resistance, from *Eq*. 6: [69]

$$I_{lim} = nFSD^{1/2}C^b \tag{6}$$

Where $I_{lim}$ is the limiting value achieved for $I_1$ when the potential is driven to a sufficiently extreme value past the peak, and the other terms have their usual meanings. The diffusion coefficient was also determined from a simple and accurate method *via* combination between the definition of both limiting convoluted current and peak current of the cyclic voltammogram using *Eq*. 7:[65]

$$I_{lim} = i_p/3.099\,(\alpha n_a v)^{1/2} \tag{7}$$

*Table* 4. Peak characteristics of the first peak of DEAC laser dye extracted from cyclic, deconvolution transforms voltammetry and digital simulation techniques at 0.1 V $s^{-1}$.

| | | |
|---|---|---|
| $E_p - E_{p/2}$, mV | 76.5[a] | 76.7[c] |
| $W_p$, mV | 112[b] | 111.8[c] |
| $\Delta E_{p\ deconv.}$ mV | 74[b] | 85[c] |
| $e_{pf}/e_{pb}$ (deconv) | 1.0[b] | 1.0[c] |

[a]Values determined from CV. [b]Values determined from deconvolution. [c]values determined from digital simulation.

where $i_p$ is the peak current, and the other parameters have their usual meanings. The $I_1$ convolution of the investigated system illustrated in *Fig*. 10 shows a distinct separation between the forward and reverse sweep and clearly indicates the sluggishness of electron transfer of the reduction process. At all sweep rates, the reverse sweep of the $I_1$ convolution return to zero due to the absence of chemical reaction at time scale of the experiments. Values of the diffusion coefficient $D$ evaluated *via Eqs* 6 & 7 are listed in *Table* 3.

The deconvolution transforms gives a rapid assessment of either the electron transfer regime or value of $E^{o'}$. Also, as shown in *Fig*. 11, the equality of peak heights of the forward and backward sweep of deconvoluted current ($e_{pb}/e_{pf}$) gives strong evidence for the simple electron transfer scheme. The mean values of the cathodic ($E_{pc(decon)}$) and the anodic ($E_{pa(decon)}$) peak potentials were taken as the redox potentials ($E^{o'}$) of the system under consideration. The estimated values of $E^{o'}$ is given in *Table* 3.

The cathodic half-peak width ($w^p$) was taken as a route for knowing the nature of electron transfer. The values of $w^p$ shown in *Table* 4 confirm the quasi-reversibility of the system under consideration.

The diffusion coefficient was also determined from deconvolution transforms using *Eq*. 8:[64]

$$e_p = \frac{\alpha n^2 F^2 v C D^{1/2}}{3.367\, RT} \tag{8}$$

where $e_p$ is the peak height (in Ampere) of the forward deconvolution sweep and the remaining terms have their usual meanings. Values of the diffusion coefficient estimated from this method are given in *Table* 3.

Also from combination between convolution and deconvolution transforms the following relationship was deduced:

$$n = \frac{e_p\ 3.367\ RT}{\alpha\ F\ v\ I_{lim}} = \frac{0.086\ e_p}{I_{lim}\ \alpha F\ \boldsymbol{v}} \tag{9}$$

where n is the number of electrons consumed in electrode reaction, the other symbols have their usual definitions. From *Eq*. 9 the number of electrons was calculated and found to be 1.1 ≈ 1.0 for the first peak and 1.03 ≈ 1.0 for the second one. As shown the number of electrons was determined without knowing the electrode surface area which considers a good, precise and simple method for determination of the number of electrons involved in the electrode reaction *via* convolution-deconvolution voltammetry.

## CONCLUSION

From our study we concluded that DEAC has high photostable in non-chlorinated solvents, undergoes solubilization in cationic and anionic micelles. DEAC displays formation of non-emissive exciplex with some organic acceptors.

DEAC was studied electrochemically *via* cyclic voltammetry, convolutive voltammetry combined with digital simulation. It was found that, the electroreduction of DEAC in 0.1 mol $L^{-1}$ TBAP/$CH_3CN$ proceeds as EE mechanism. The first charge transfer produces monoanion radical while the second charge transfer produces dianion. Digital simulation was used to confirm the electrochemical parameters and the electrode nature of the investigated system.

## REFERENCES


1. Fletcher, A. N.; Biss, D. E. *Appl. Phys*. **1978**, *16*, 289.
2. Atkins, R. L.; Biss, D. E . *J. Org. Chem*. **1978**, *43*, 1975.
3. Halstead, J. A.; Reeves, R. R. *Opt. Commun*. **1987**, *27*, 273.
4. Fletcher, A. N. *Appl. Phys*. **1977**, *14*, 295.
5. Schimitschek, E. J.; Trias, J. A.; Hammond, P. R.; Henry, R. A.; Atkins, R. L. *Opt. Commun*. **1975**, *13*, 313.
6. Reynolds, G. A.; Drexhage, K. H. *Opt. Commun*. **1975**, *13*, 222.
7. Duart, F. J., Hilman, L. W. Eds.; *Dye Laser Principles with Application*; Academic Press: New York, 1990; p 390.
8. Azim, S. A.; Al-Hazmy, S. M.; Ebeid, E. M.; El-Daly, S. A. *Optics and laser Technology* **2005**, *37*, 245.
9. Rechthaler, K.; Kohler, G. *Chem. Phys.* **1994**, *189*, 99.
10. Jones, G.; Feng, Z.; Bergmark, W. R. *J. Phys. Chem*. **1994**, *98*, 4511.
11. Jones, G.; Jackson, W. R.; Halpern, A. M. *Chem. Phys. Lett*. **1980**, *72*, 391.
12. Jones, G.; Jackson, W. R.; Konaktanaporn, S. *Opt. Commun*. **1980**, *33*, 315.
13. Jones, G.; Jackson, W. R.; Choi, C. Y.; Bergmark, W. R. *J. Phys. Chem*. **1985**, *89*, 294.
14. Sarkar, N.; Das, K.; Dutta, A.; Bhattacharyya, K. *J. Phys. Chem*. **1996**, *100*, 15483.
15. Sarkar, N.; Das, K.; Dutta, A.; Das, S.; Bhattacharyya, K. *J. Phys. Chem*. **1996**, *100*, 10523.
16. Gardecki, J. A.; Maroncelli, M. *J. Phys. Chem*. **1999**, *103*, 1187.
17. Horng, M. L.; Gardecki, J.; Papazyan, A.; Maroncelli, M. *J. Phys. Chem*. **1995**, *99*, 17311.
18. Atanu, B.; Sukhendu, N.; Haridas, P. J. *Chem. Phys*. **2003**, *119*, 10202.
19. Maroncelli, M. *J. Mol. Liq*. **1993**, *57*, 1.
20. Chapman, C. F.; Maroncelli, M. J. *Phys. Chem*. **1991**, *95*, 9095.
21. Nad, S.; Kumbhakar, M.; Pal, H. J. *Phys. Chem. A* **2003**, *107*, 4808.
22. Harle, A. J.; Lyons, L. E. *J. Chem. Soc.* **1950**, 1575.
23. Capka, O. *Czech. Czech. Chem. Commun*. **1950**, *15*, 965.
24. Zuman, P. *Chem. Listy*. **1954**, *48*, 94.
25. Zuman, P. *Organic Polarographic Analysis*; Pergamon Press: New York, 1964; p 251.
26. Zuman, P. *Substituent Effects in Organic Polarography*; Plenum Press: New York, 1967; p 165.
27. Gourley, R. N.; Grimshaw, J.; Miller, P. G. *J. Chem. Soc.(C)* **1970**, 2318.
28. Reddy, B. O.; Reddy, A. V.; Raju, K. M.; Rao. A. K. *J. Electro Chem. Soc. India* **1989**, *35*, 319.
29. Partridge, L. K.; Tansley, A. C.; Porter, A. S. *Electrochem. Acta*. **1966**, *11*, 517.
30. Bond, A. M.; Thomas, F. G. *Langmuir*. **1988**, *4*, 341.
31. Helin, M.; Jiang, Q.; Ketamo, H.; Hakansson, M.; Spehar, A. M.; Kulmala, S.; Ala-Kleme, T. *Electrochimica Acta.* **2005**, *51*, 725.
32. Carrazon, J. M. P.; Vergara, A. G.; Garcia, A. J. R.; Diez, L. M. P. *Anal. Chim. Acta*. **1989**, *216*, 231.
33. Dempsey, E.; O'Sullivan, C.; Smyth, M. R.; Egan, D.; O'kennedy, R.; Wang, J. *J. Pharm. Biomed. Anal*. **1993**, *11*, 443.
34. Dempsey, E.; O'Sullivan, C.; Smyth, M. R.; Egan, D.; O'kennedy, R.; Wang, J. *Analyst*. **1993**, *118*, 411.
35. Wu, Q.; Dewald, H. D. *Electroanalysis*. **2001**, *13*, 4.
36. Melhuish, W. H. J. *Phys. Chem*. **1960**, *64*, 762.
37. Morris, J. V.; Mahany, M. A.; Huber, I. R. J. *Phys. Chem*. **1976**, *80*, 971.
38. Ebeid, E. M.; Issa, R. M.; Ghoneim, M. M.; El-Daly, S. A. *J. Chem. Soc. Faraday Trans*. *1* **1986**, *82*, 909.
39. Murov, S. L. *Hand Book of Photochemistry*, Marcel Dekker, New York, **1973**, p 119.
40. Rajiv, B. B.; Costa, M. B. *Phys Chem. Chem. Phys*. **1999**, *1*, 3539.
41. Andre, J. C.; Nicolas, M.; Ware, W. R. *Chem. Phys*. **1978**, *28*, 371.
42. Frolicker, R. *J. Phys. Chem. A*. **2002**, *106*, 1708.
43. Supine, P. *J. Photochem. Photobiol. A: Chem*. **1990**, *50*, 293.
44. Lapper, E. Z. *Electromchem. Soc.* **1957**, *61*, 962.
45. El-Daly, S. A.; Garber, M.; Shihry, S. S.; El-Sayed, Y. S. *J. Photochem. Photobiol. A: Chem*. **2008**, *195*, 89.
46. Matera, N.; Kubota, T. *Molecular interaction and electronic spectra* Marcel Dicker, New York, 1970.
47. Broks, J. B. *Photphysics of Aromatic molecules*, Wiley Interscience; New York, 1970.
48. Gordon, P.; Gregory, P. *Organic Chemistry in Color*, Moskva: Chimia, 1987.
49. Eicke, H. F. Top. *Curd. Chem*. **1980**, *87*(1), 86.
50. Fendler, J. H. *J. Phys. Chem*. **1980**, *84*, 1485.
51. deValle, J. C.; Kasha, M.; Catalan, J. *J. Phys. Chem. A*. **1997**, *101*, 3260.
52. Beaumont, I. C.; David Johnson, G.; Barry Parsons, B. J. *J. Chem. Soc. Faraday Trans*. **1993**, *89*, 4185.
53. Antoniou, V. S.; Holed, K. L. *Appl. Phys. B*. **1983**, *32*, 9.
54. Bionics, M. C.; Balsells, R. E. *J. Photochem. Photobiol. A: Chem*. **1994**, *77*, 149.

55. Mastsuda, M. C. S.; Kokado, R. H.; Inoue, E. *Bull. Chem. Soc. Jpn*. **1970**, *43*, 2994.
56. Balsells, R. E.; Farsca, A. *Aust, J. Chem*. **1988**, *41*, 104.
57. Wolinski, L.; Turzynski, Z.; Witkowaski, K. *Markromol. Chem*. **1987**, *188*, 2895.
58. Bard, A. J.; Ledwith, A.; Shine, H. J. *Adv. Phys. Org. Chem*. **1976**, *12*, 155.
59. El-Daly, S. A.; Fayed, T. A. *J. Photochem. Photobiol. A: Chem*. **2000**, *137*, 15.
60. Azim, S. A.; El-Daly, H. A.; El-Daly, S. A.; Zeid, K. A.; Ebeid, E. M.; Heldt, J. R. *J. Chem. Soc. Faraday Trans*. **1996**, *92*(5), 2685.
61. Kavarnos, G. J.; Turro, N. *J. Chem. Rev*. **1986**, *86*, 401.
62. Nichlson, R. S. *Anal. Chem*. **1965**, *37*, 1351.
63. Bard, A. J.; Faulkner, L. R. *Electrochemical Methods, Fundamentals and Applications*, Wiley, New York, **1980**.
64. El-Daly, S. A.; El-Hallag, I. S.; Ebeid, E. M.; Ghoneim, M. M. *Chin. J. Chem*. **2009**, *27*, 241.
65. El-Hallag, I. S.; Ghoneim, M. M.; Hammam, E. *Anal. Chim, Acta*. **2000**, *414*, 173.
66. El-Hallag, I. S.; Hassanien, A. M. *Collect. Czech. Chem. Commun*. **1999**, *64*, 1953.
67. El-Hallag, I. S.; Ghoneim, M. M. *Monatsh. Chem*. **1999**, *130*, 525.
68. Ammar, F.; Saveant, J. M. *J. Electroanal. Chem*. **1973**, *47*, 215.
69. Imbeaux, J. C.; Saveant, J. M. *J. Electroanal. Chem*. **1973**, *44*, 169.
70. Dobson, I. D.; Taylor, N.; Tipping, L. R. H. in *Electrochemistry, Sensor and Analysis*, **1986**, pp 61-75. Elsevier. Amsterdam.
71. Ghoneim, M. M.; El-Hallag, I. S. *Monatsh. Chem*. **1999**, *130*, 525.
72. Oldham, K. B. *Anal Chem*. **1983**, *9*, 145.
73. El-Hallag, I. S.; Hassanein, A. M.; Ghoneim, M. M. *Monatsh. Chem*. **1995**, *126*, 1075.